PCCP

RSC Publishing

PAPER

View Article Online
View Journal | View Issue

Cite this: Phys. Chem. Chem. Phys., 2013, 15, 2684

Coherent transient spectroscopy with continuous wave quantum cascade lasers

James M. R. Kirkbride,[a] Sarah K. Causier,[a] Elin A. McCormack,[a] Damien Weidmann[ab] and Grant A. D. Ritchie*[a]

Received 19th November 2012, Accepted 4th January 2013

DOI: 10.1039/c2cp44116k

www.rsc.org/pccp

A high power continuous wave quantum cascade laser operating around 1900 cm^{-1} has been used to conduct Lamb dip spectroscopy on a low pressure sample of NO. The widths of the Lamb dips indicate that the laser linewidth is 800 $\pm$ 60 kHz and the power sufficient to induce significant population transfer of up to 35%. While the Lamb dip signals are symmetric at low laser chirp rates, they become increasingly asymmetric as the chirp rate increases, further confirming the significant degree of population transfer. In addition rapid passage structure on the Lamb dip signal is observed after the weak probe beam is swept through the line center. This structure is sensitive to both the probe chirp rate and the underlying hyperfine structure of the rovibrational transition, and is accurately modeled using the optical Bloch equations.

1 Introduction

Recent advances in quantum cascade laser (QCL) design have enabled the production of high powered single mode continuous wave (cw) lasers with narrow linewidths.[1–4] These are ideal sources not only for sensing strategies based on modulation spectroscopy such as wavelength modulation spectroscopy (WMS) and cavity enhanced absorption and ringdown spectroscopies (CEAS, CRDS), but also for non-linear spectroscopy and vibrational state preparation. For pulsed QCLs application of a current pulse to the laser results in rapid Joule heating causing a fast frequency down chirp in the laser output. The resulting high chirp rate may mean that the laser is swept through a spectroscopic resonance in a sample of low pressure gas in a time that is short compared to that for collisionally induced polarization dephasing. Under these conditions, the macroscopic polarization of the sample can beat with the chirping laser field to modify the transmission (or emission) function of the sample – this is the coherent transient effect known as rapid passage. Studies using pulsed QCLs show that rapid passage leads to considerable oscillatory structure post resonance in the absorption spectrum provided that the detector/amplifier system has sufficient bandwidth to resolve the high oscillation frequency.[5,6] Similarly by applying a waveform to a cw QCL the frequency may be scanned, with the rate depending on the frequency and magnitude of the applied waveform. Rapid passage was recently observed in a velocity selected sample of NO using two cw QCLs in a pump–probe type setup,[7] and in a single laser setup over a long path length using OCS gas.[8] Other coherent effects may also be seen with rapidly chirped QCLs such as the electric field induced Autler–Townes splitting seen by Duxbury *et al.*[9,10] In this case the splitting, observed in a low pressure sample of NO over a pathlength of 100 m, was found to be laser chirp rate dependent.

At low pressures (less than 1 Torr) the Doppler effect causes an inhomogeneous broadening of the molecular absorption line, producing a Gaussian lineshape with a full-width at half maximum of *ca.* 130 MHz in the mid IR for NO. Since each hyperfine transition is broadened by this amount it is not generally possible to resolve the individual lines using standard absorption spectroscopy. Sub-Doppler resolution of a spectral line may be achieved by reducing the size of the velocity group being probed. For instance using Lamb dip spectroscopy.[11] For this work, velocity profile selection was achieved by using two beams formed by a beam splitter which gives *ca.* 90% of the laser power in a pump beam and allows a high level of spatial overlap between the pump and the remaining 10% of the power in the probe beam. The laser is scanned over the transition of interest by applying a triangular voltage ramp to the current driver in order to produce small changes in the input current. Since the two beams counter propagate and scan through the same frequencies simultaneously, they interact with velocity groups that have equal and opposite velocity components along

[a] Department of Chemistry, University of Oxford, Physical and Theoretical Chemistry Laboratory, South Parks Road, Oxford, OX1 3QZ, UK. E-mail: grant.ritchie@chem.ox.ac.uk; Fax: +44 (0)1865 275410; Tel: +44 (0)1865 285723

[b] Space Science and Technology Department, STFC Rutherford Appleton Laboratory, Harwell Oxford Campus, Didcot, OX11 0QX, UK

the z axis (defined as the direction of propagation of the pump beam). The two beams can only interact with the same molecular velocity group when there is zero velocity component in the z direction. At this frequency the pump beam excites the molecules into the upper state and the gas becomes partially transparent to the probe beam resulting in a dip in the measured absorption at the line center. The width of the Lamb dip is determined by the transit time and self broadening parameter of the molecules, and by the laser linewidth. At low pressure both the transit time broadening and the self broadening are on the order of a few kHz so the width of the Lamb dip is usually dominated by the laser linewidth and as such can be used as a measurement of said property. For a strong saturating pump wave and a weak counter-propagating probe the form of the absorption coefficient for a Lamb dip spectrum is given by eqn (1),[12]

$$\begin{aligned}\alpha(\omega) &= \alpha^0(\omega)\left[1-\left(1-\frac{1}{\sqrt{1+S_0}}\right)\frac{\Gamma^2}{\Gamma^2+(\omega-\omega_0)^2}\right],\\ \Gamma &= \frac{\gamma}{2}\left(1+\sqrt{1+S_0}\right), \qquad (1)\\ S_0 &= \frac{2|\mu|^2 I_\mathrm{p}}{c\varepsilon_0 h^2\gamma^2},\end{aligned}$$

in which $\alpha^0(\omega)$ is the unsaturated Doppler profile, ω is the laser frequency, ω_0 is the center frequency of the transition, γ is the relaxation rate of the system, μ is the transition dipole moment, I_p is the intensity of the pump laser and S_0 is the saturation parameter. The signal measured at the detector is a convolution of eqn (1) with a Gaussian function representing the frequency distribution of the laser. An analytical approximation to this convolution is given by Mukherjee *et al.* assuming that the laser linewidth is larger than the power broadened homogeneous width,[13]

$$\alpha(\omega) = \alpha_\mathrm{p}\left[\mathrm{e}^{-\left(\frac{\omega-\omega_0}{\Delta_\mathrm{D}}\right)^2} - \frac{\sqrt{\pi}\Gamma}{\Delta_\mathrm{l}}\left(1-\frac{1}{\sqrt{1+S_0}}\right)\mathrm{e}^{-\left(\frac{\omega-\omega_0}{\Delta_\mathrm{l}}\right)^2}\right], \qquad (2)$$

where α_p is the maximum absorbance (*i.e.* at line centre), Δ_D is the Doppler width and Δ_l is the laser linewidth. The first term in the brackets represents the unsaturated Doppler absorption profile *i.e.* a Gaussian function, and the second the Lamb dip broadened by the laser linewidth. This model will be used in experimental data interpretation.

This paper presents examples of coherent effects seen in the fundamental rovibrational absorption spectrum of NO at *ca.* 5 μm and their effects on Lamb dip signals. More specifically, two rotationally resolved transitions within the $\nu = 1 \leftarrow 0$ vibrational band of the ground $^2\Pi$ electronic state are investigated. The two transitions studied, $\mathrm{R}(6.5)_{\frac{1}{2}}$ and $\mathrm{R}(6.5)_{\frac{3}{2}}$, have the same total angular momentum quantum number (J = 6.5) but differ in their spin orbit states $\left(\Omega = \frac{1}{2}, \frac{3}{2}\right)$. The two transitions display slightly different structure owing to differing splittings caused by hyperfine interactions with ^{14}N, and Λ doubling caused by the rotation of the molecule lifting the orbital angular momentum degeneracy. The hyperfine splitting is the smaller of these two effects. The $\mathrm{R}(6.5)_{\frac{3}{2}}$ transition displays the larger hyperfine splitting and is used to measure the laser linewidth, and the $\mathrm{R}(6.5)_{\frac{1}{2}}$ transition is investigated to study coherence effects.

2 Experimental

The work was carried out using a Maxion M575AH-NS single mode cw distributed feedback (DFB) QCL housed in an in-house designed mount and cooled by a two stage peltier thermoelectric cooler. The laser was then driven by a custom designed low noise current source. The laser emits over the range 1897–1904 cm^{-1} with powers up to 250 mW. The beam is split by a CaF_2 beam splitter and the pump and probe beams then counter propagate through a 112 cm long cell fitted with Brewster angled CaF_2 windows. The probe beam is collected onto a detector (VIGO PVMI-3TE-10.6) while the pump beam goes to a beam dump. The ideal alignment of the system would have the pump and probe beams perfectly overlapping, however this causes optical feedback into the laser which induces mode hops when the laser is scanned. Therefore the setup must be slightly misaligned such that there is sufficient overlap to observe Lamb dips but without causing significant optical feedback (Fig. 1).

The laser frequency was scanned by applying a triangular voltage ramp to the current controller using a digital function generator (TTi TG1304). The laser chirp rate is a function of both the frequency and amplitude of the voltage modulation. The spectra were recorded using a 400 MHz bandwidth digital oscilloscope (LeCroy WaveSurfer 44MXs-A). All data was recorded on a frequency up-chirp and approximately 100 sweeps were recorded with the data subsequently being re-centered on the minimum of the Lamb dip and averaged in MATLAB to reduce drifts and noise. A frequency scale is established using the positions of the Lamb dips as known fixed frequency points and interpolating across the Doppler broadened background spectrum. The chirp rate is calculated using a germanium etalon with a free spectral range (FSR) of 500 MHz. The transmission function of the etalon as the laser frequency is

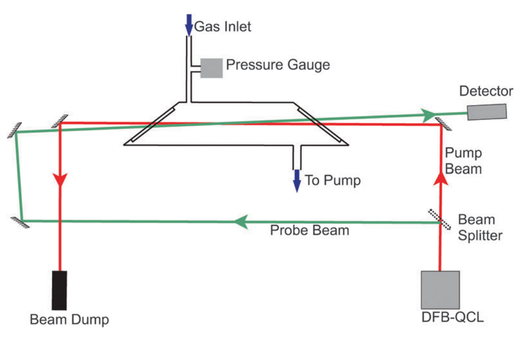

Fig. 1 Lamb dip experimental setup. The beam is split into 'pump' and 'probe' beams which counter propagate through the cell.

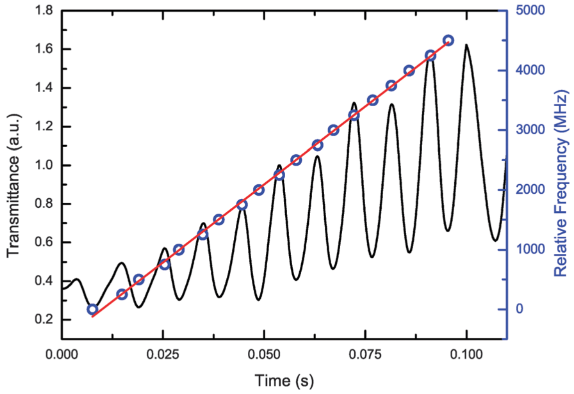

Fig. 2 The transmission of the germanium etalon during a frequency up-chirp of the laser, shown with a linear fit to the time spacing of the fringes (frequency spaced by the FSR of 500 MHz) giving a frequency chirp rate of 0.053 MHz μs^{-1}.

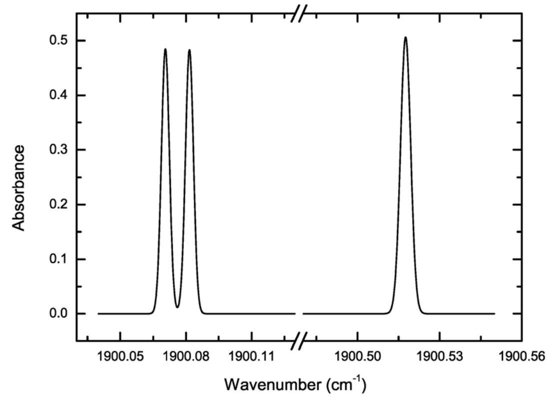

Fig. 3 Calculated absorption spectrum of NO covering both spin-orbit states of the R(6.5) ν = 1 ← 0 transition. The transition originating from the $\Omega = \frac{1}{2}$ spin-orbit state appears as a doublet due to Λ doublet splitting, whereas that from the $\Omega = \frac{3}{2}$ state appears as a singlet as the Λ doublet splitting is less than the Doppler width. The calculations were made using the absorption cross sections given by HITRAN.[14]

scanned appearing in Fig. 2 shows that the frequency scan is nearly linear and as such the frequency scale is directly given by the spacing of the transmission maxima in the time-domain signals. The change in amplitude of the fringes and the ramped baseline reflect the small change in power of the laser across the current scan.

3 Results and discussion

Laser linewidth measurements

The orbital angular momentum quantum number L is poorly defined in the ground electronic state of NO and instead the projection of L onto the internuclear axis, Λ, is used. For NO, $\Lambda = \pm 1$ leads to two degenerate states which are split by the rotation of the nuclear framework; an effect known as Λ-doubling. The two resulting non-degenerate states are labeled e and f and the transitions originating from each, and terminating in the same Λ-doublet components in the ν = 1 state, are separated by *ca.* 330 MHz and *ca.* 26 MHz in the $\mathrm{R}(6.5)_{\frac{1}{2}}$ and the $\mathrm{R}(6.5)_{\frac{3}{2}}$ transitions respectively. Hence in an absorption spectrum the $\mathrm{R}(6.5)_{\frac{1}{2}}$ transition appears as a doublet whereas in the $\mathrm{R}(6.5)_{\frac{3}{2}}$ transition the splitting is less than the Doppler broadening and it appears as a singlet as shown in Fig. 3. There is a further splitting due to hyperfine coupling with the nuclear spin of the nitrogen (I = 1). Each angular momentum state is thus split into three hyperfine levels, giving a total of six hyperfine levels. The selection rule for transitions between these hyperfine levels is $\Delta F = 0, \pm 1$ where $F = |J + I| \cdots |J - I|$ is the total angular momentum quantum number including nuclear spin. For the transitions studied $\Delta J = +1$ and the strongest absorptions are for $\Delta F = +1$ leading to three strong absorption lines spaced by between 0.1 and 3.1 MHz in each Λ-doublet.

The laser linewidth was measured using Lamb dip spectroscopy on the NO $\mathrm{R}(6.5)_{\frac{3}{2}}$ ν = 1 ← 0 transition. The cell was filled with approximately 8 mTorr of NO and a Lamb dip spectrum was recorded at a laser chirp rate of 0.053 MHz μs^{-1} with a pump power of 130 mW. Six hyperfine lines were apparent in the resulting spectrum shown in Fig. 4. This data was fitted with eqn (2) using least squares minimisation in MATLAB. The equation is applied to all six hyperfine transitions with the amplitudes of the Doppler profiles being weighted according

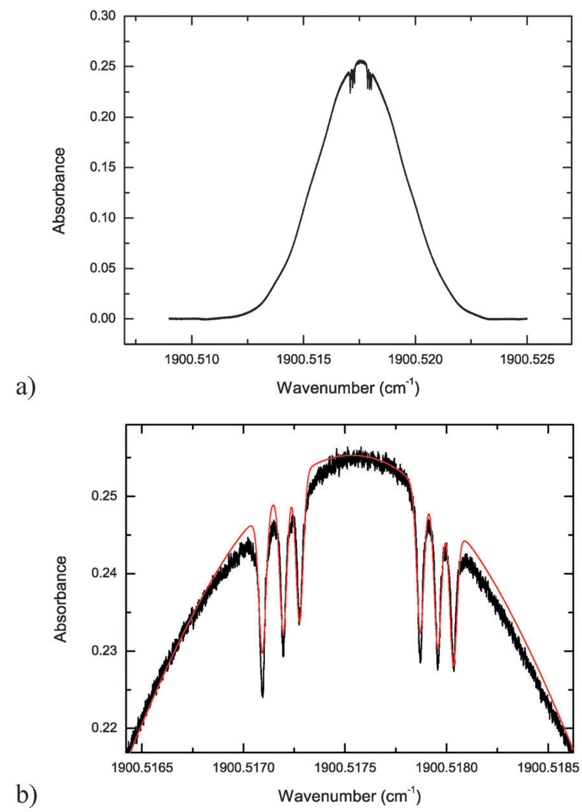

Fig. 4 Lamb dip spectrum of the NO $\mathrm{R}(6.5)_{\frac{3}{2}}$ ν = 1 ← 0 transition showing 6 separate Lamb dips corresponding to the strongest 6 hyperfine transitions. The full Doppler profile is shown at a pressure of *ca.* 8 mTorr and a laser chirp rate of 0.053 MHz μs^{-1} in (a). The fit to the observed spectrum using eqn (2) which gave a laser linewidth of 800 ± 60 kHz is shown in (b).

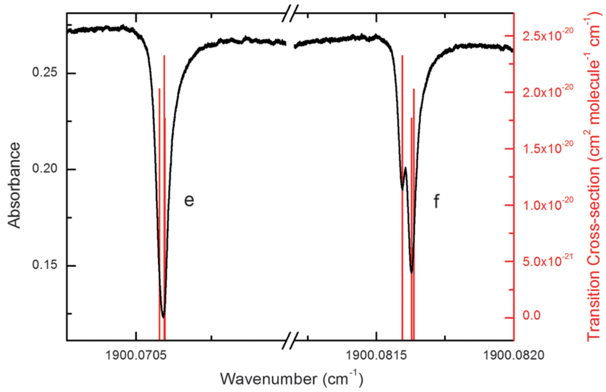

Fig. 5 Lamb dip spectra of the *e* and *f* components of the Λ doublet in the $\mathrm{R}(6.5)_{\frac{1}{2}}$ transition of NO with the transition intensities (from HITRAN[14]) of the corresponding hyperfine components shown. Note that the laser linewidth is narrow enough to allow partial resolution of the hyperfine lines in the *f* component.

the transition cross sections given by HITRAN,[14] and the saturation parameters weighted according to the squares of the respective dipole moments. The overall Doppler lineshape is the sum of the six individual components. The fit to the data in Fig. 4a is shown in Fig. 4b. The Lamb dips are well fit by the Gaussian lineshape in the second term of eqn (2) with full-width at half-maximum giving a laser linewidth of 800 $\pm$ 60 kHz. This compares favourably with linewidths of 21 MHz,[13] 4 MHz,[15] and 2.5 MHz measured using similar techniques with external cavity QCLs.[16] The linewidth is limited mainly by supply current noise since the intrinsic linewidth of QCLs has been shown to be of the order of only a few hundred Hz.[2,17] The effects detailed in the rest of this paper resulted in the 6 Lamb dips seen on the $\mathrm{R}(6.5)_{\frac{3}{2}}$ transition blurring into one another. As a result transient experiments were carried out on the $\mathrm{R}(6.5)_{\frac{1}{2}}$ transition in which the hyperfine splitting in each Λ-doublet cannot be resolved. Only a single Lamb dip is seen on each of the Λ-doublet peaks (see Fig. 5). Due to the narrow linewidth of the laser it is however possible to partially resolve one of the hyperfine transitions (with a splitting of 1.02 MHz) in the *f* component from the other two, but in the *e* component the splitting is much less than the laser linewidth and so only a single dip is observed.

Lamb dip shape as a function of chirp rate

For lower chirp rates the depth of Lamb dips was observed to increase relative to the size of the absorption signal as the chirp rate increased. Fig. 6 shows examples of this behaviour. The Lamb dips were again fitted using eqn (2). The values of γ and Δ_1 were both fixed parameters in the fitting with γ calculated from the quadrature addition of the transit time broadening and the collisional broadening and the laser linewidth being fixed at the measured value of 800 kHz. Again all six hyperfine components are summed to give the overall lineshape. The increase in the size of the Lamb dip reflects an increase in the population transferred into the $\nu = 1$ level as plotted in Fig. 7. The population transfer is seen to increase from around 20% to over 35%, simply by increasing the chirp rate.

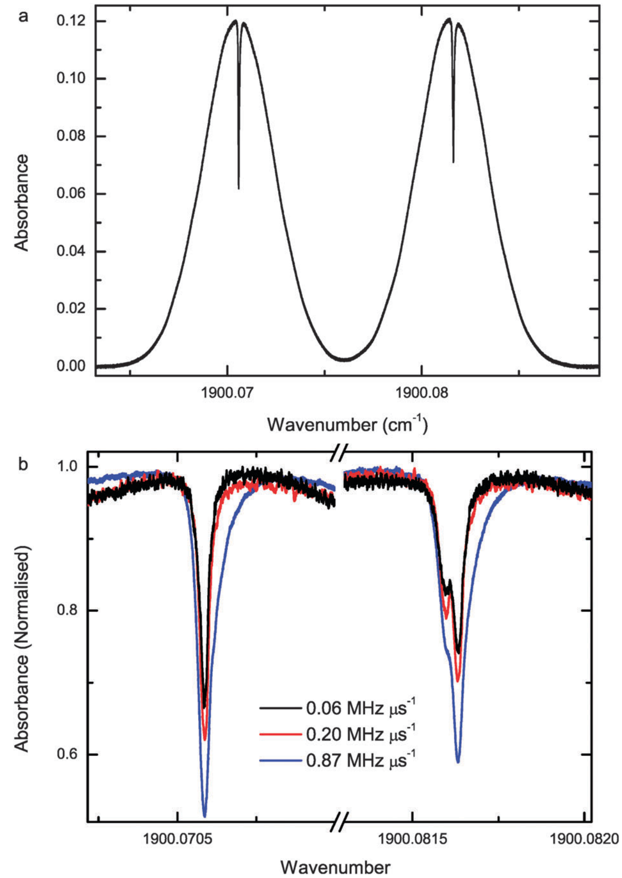

Fig. 6 The full Doppler profile for the *e* and *f* components of the $\mathrm{R}(6.5)_{\frac{1}{2}}$ transition with two Lamb dips is shown in (a) for the $\mathrm{R}(6.5)_{\frac{1}{2}}$ transition at a chirp rate of 0.87 MHz μs^{-1}. The effect of increasing chirp rate on the size of the Lamb dip is shown in (b).

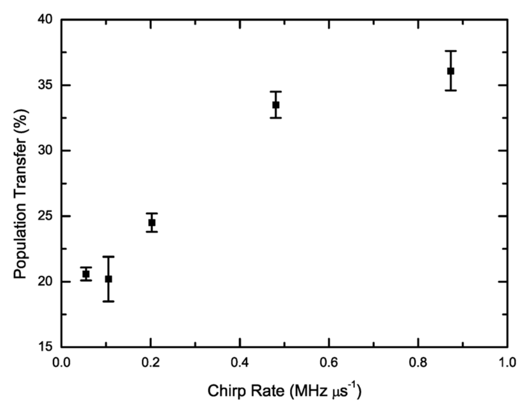

Fig. 7 Population transfer as a function of chirp rate.

This effect of chirp rate on the magnitude of the Lamb dip was previously observed by Hamadani *et al.* in a low pressure sample of NH_3 pumped with a high power N_2O laser.[18] In their study they found that at appropriately high chirp rate the Lamb dips switched to amplification indicating an inversion of population. This is evidence for adiabatic rapid passage (ARP)

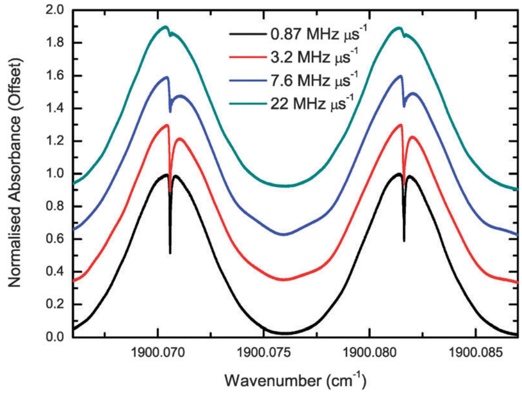

Fig. 8 Increasingly asymmetric Lamb dip spectra are seen as the chirp rate is increased. All data was taken with 10 mTorr NO and data sets have been offset for clarity.

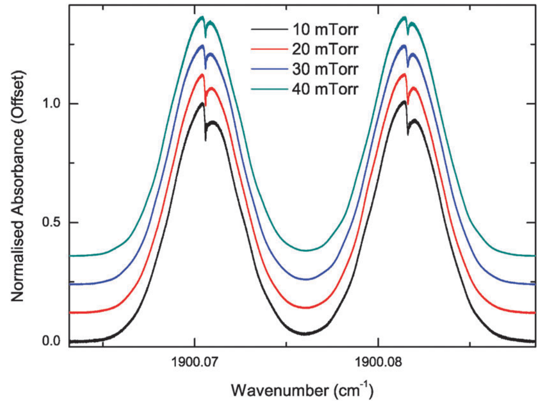

Fig. 9 The variation in the asymmetric Lamb dip spectra as a function of pressure. As the pressure increases the dips get smaller in proportion to the background absorption profile and become more symmetric. All data was taken at laser chirp rate of 7.7 MHz μs^{-1} and the profiles were normalized and offset for clarity.

where the definition of 'rapid' is that the laser is swept through resonance in a time that is short compared to the collisional relaxation of the gas. In their study the laser intensity was significantly higher (5 W cm^{-2}) than in the present study (1 W cm^{-2}), explaining why amplification is not seen in our data.

Raising the chirp rate above about 0.9 MHz μs^{-1} however does not lead to further increases in the magnitude of the Lamb dips and in fact they become noticeably asymmetric. The absorbance post resonance in the probe scan becomes lower than expected for the Doppler profile as shown in Fig. 8. This asymmetry is independent of the direction of frequency scan *i.e.* for the case of a frequency up chirp it occurs to higher frequency than the line centre but on a down chirp the asymmetry lies to lower frequency. The magnitude of the dip also decreases with increasing chirp rate as the asymmetry increases. The cause of this asymmetry relates to the counter-propagating nature of the experiment. As the probe laser passes through the center of the Doppler broadened line where $\omega_{probe} = \omega_0$ it begins to interact with velocity groups that have already been pumped. These velocity groups have a significant amount of population in the $\nu = 1$ state when pumped. Hence the population difference ΔN, to which the absorbance is proportional, is reduced compared to those that are probed pre-Lamb dip. The population of the $\nu = 1$ state may decay in the time period between being pumped and being probed. The length of time between pumping and probing for each velocity group depends on the chirp rate of the laser, thus the faster the laser is scanned, the less time the population in the $\nu = 1$ state has to decay. This is entirely as expected for a system in which the main method of depopulating the upper state is molecular collisions. The asymmetric line shape, to a first approximation, can be thus fitted using eqn (3),

$$\alpha = \alpha_0(1 - Ae^{-kt}), \tag{3}$$

where t is the time taken between a velocity group being pumped and the probe laser interacting with it, A is proportional to the initial amplitude of the Lamb dip, and k is a phenomenological decay constant which quantifies depopulation (and dephasing) of the upper state. Eqn (3) was convolved with a Gaussian of full-width at half-maximum 800 kHz, representing the laser linewidth function and fitted to the data using least squares fitting in a MATLAB program. The fitting routine applies in the post-resonance regime since before this point the probe beam only sees molecules that have not been pumped, and we therefore define t to be zero pre-resonance. The decay constant, k, is found to be approximately equal to the collision frequency within the gas sample. As well as a change in the asymmetry with chirp rate, there is a noticeable change with pressure as shown in Fig. 9. The dips get smaller and the spectra more symmetric with increasing pressure, reflecting the increasing importance of collisional relaxation of the $\nu = 1$ population. In Fig. 8 and 9 the Doppler broadened absorption profiles have been normalized to show how the size of the dip changes relative to the background absorption.

Rapid passage

The asymmetry in the Doppler profile was fit using eqn (3) and a least squares minimisation program in MATLAB. A fit to the e component of the $R(6.5)_{\frac{1}{2}}$ transition at a chirp rate of 18 MHz μs^{-1} is shown in Fig. 10. In general the overall functional form of the data is well fitted using this model. A closer examination of the Lamb dip reveals oscillations post-resonance as shown in the inset to Fig. 10. These oscillations occur *only* after the probe laser has scanned through the line center, to later time in the scan. Again, the oscillations are seen to later time regardless of whether the probe laser is scanning to increasing or decreasing frequency. The oscillatory structure resembles the rapid passage signals seen using chirped pulsed QCLs; the electric field produced by the polarized vibrationally excited molecules interferes with the electric field of the scanning probe laser and causes the intensity oscillations seen. The process happens on a timescale that is short compared with the relaxation time of the system and as such the rapid passage does not appear at very slow laser scan rates below

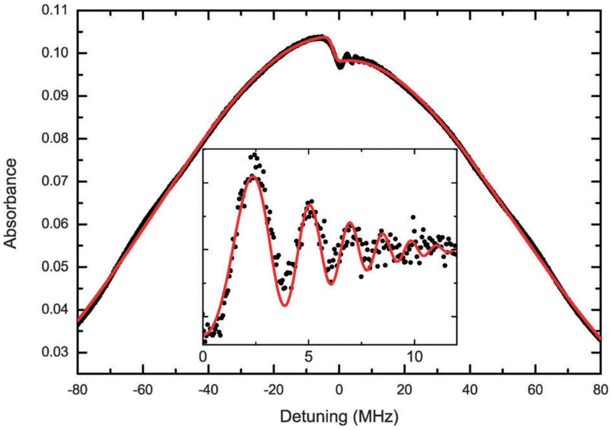

Fig. 10 A fit to the e component of the $R(6.5)_{\frac{1}{2}}$ transition at a chirp rate of 18 MHz μs^{-1} using eqn (3) is shown with the rapid passage oscillations post-resonance shown inset. The rapid passage oscillations are fit by a model which solves the optical Bloch equations. The signals are plotted against the detuning from the center frequency of the Lamb dip.

about 4 MHz μs^{-1}. As with our previous work in a pump probe experiment,[7] we find that the rapid passage signature is only visible due to the sub-Doppler laser bandwidth causing significant velocity selection as no such rapid passage occurs when the pump beam is blocked, removing the velocity selective pumping. Because the pumped velocity group is small (being determined by the laser linewidth) the velocity spread of the pumped molecules is very low and the molecules dephase slowly. Hence even though the laser is scanned slowly compared to the chirp rate of pulsed QCLs (*ca.* 3–4 orders of magnitude difference), the scan is still fast compared with the dephasing time of the pumped velocity group and rapid passage can be observed. This behaviour has been modeled using the optical Bloch equations using a previously described MATLAB program.[7] The model takes the properties of the molecular transition such as the dipole moment and longitudinal and transverse relaxation rate constants, and the laser intensity and interaction length and produces a simulation of the expected rapid passage oscillations. The model has been applied to the oscillations shown in the inset of Fig. 10 and shows good agreement with the experimental data. To our knowledge this is the first observation of rapid passage signals in Lamb dip spectroscopy.

The rapid passage signals for the two Λ doublet components of the $R(6.5)_{\frac{1}{2}}$ transition were found to differ in appearance. Moreover it is seen that the observed difference between the rapid passage structures on the *e* and *f* components changes depending on the chirp rate of the laser. The observed signal on the *e* component looks as expected for rapid passage, however on the *f* component there is a marked difference, attributed to the hyperfine splitting. In the *f* component the splitting as shown in Fig. 5 is sufficiently large that a rapid passage signal beginning on the partially resolved hyperfine transition may be slightly out of phase with that originating from the other two hyperfine transitions. Hence these two signals interfere and cause the change in overall signal shape that is observed. Again this effect was modeled using the optical Bloch equations as shown in Fig. 11. The three hyperfine transitions on each Λ-doublet each contribute an oscillating rapid passage signal. These signals are summed and then convolved with a Gaussian with a full width at half maximum of 1 MHz to represent the probing laser linewidth. The results of the simulations are shown in Fig. 11c and f (for *e* and *f* components respectively) and are in good qualitative agreement with the experimental data shown in Fig. 11a and d. It should be noted that these experimental data had the underlying asymmetry subtracted using the best fit from eqn (3). In addition, the simulations are

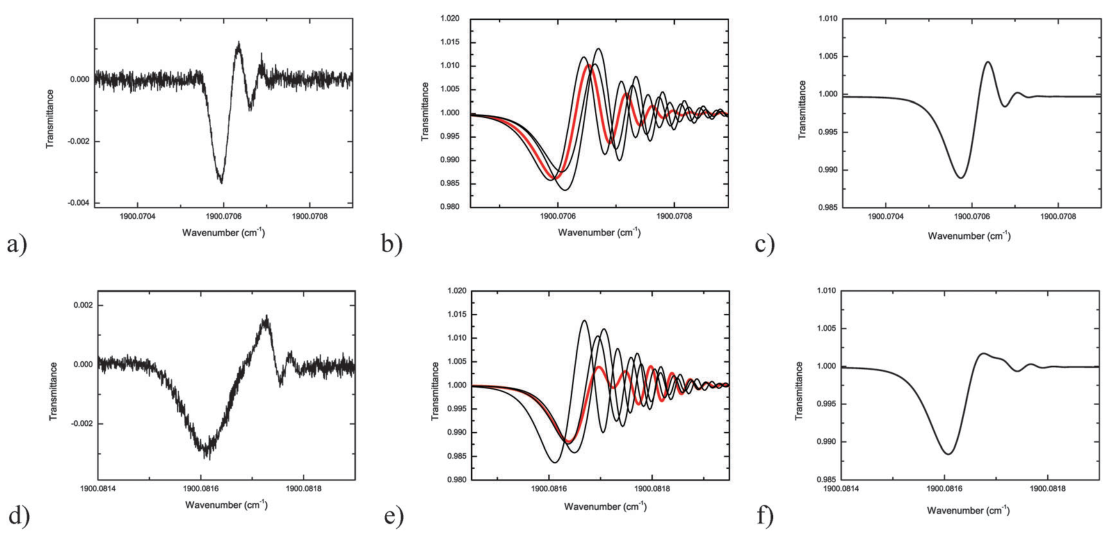

Fig. 11 Rapid passage signals at a laser chirp rate of 7.7 MHz μs^{-1} and a pressure of 9 mTorr for the $R(6.5)_{\frac{1}{2}}$ transition. (a) to (c) correspond to the e component and (d) to (f) to the *f* component. The experimental data is shown in (a) and (d) with the asymmetric Doppler profile subtracted. Images (b) and (e) show the simulations of the rapid passages signals for the three hyperfine components of the respective transitions along with their sum in bold. Finally (c) and (f) show the signal expected at the detector, calculated by convolving (b) and (e) with a Gaussian function representing the probe laser linewidth.

also in good agreement with the chirp rate dependence and shape of the experimental data for both Λ doublet components.

Single velocity group pumping

The asymmetry in the Doppler profile is due to the simultaneous frequency scan of pump and probe beams in a counter-propagating setup with significant population transfer induced by the QCL, while the rapid passage oscillations are due to the induced polarisation of the pumped molecules beating with the chirping laser field. Given this interpretation of our data, it should be possible to see rapid passage oscillations without the asymmetry by using a separate laser to pump a single velocity group within the Doppler profile. To this end a single velocity group within the Doppler profile of the $R(6.5)_{\frac{1}{2}}$ transition was pumped using a fixed frequency supplied by a second QCL (Daylight solutions external cavity QCL).[19] Due to frequency instability of the pumping Daylight QCL it was not possible to perform any averaging on the recorded data, however the lack of asymmetry in the Doppler profile makes the rapid passage oscillation even more pronounced. Fig. 12 shows a velocity group with a small component in the direction of laser propagation being pumped within the *f* component of the Λ doublet resolved transition. Rapid passage oscillations are clearly seen however the asymmetry caused by pumping all velocity sets before probing them is not.

The data shown in Fig. 12 was taken with the Maxion laser scanning at 60.5 MHz μs^{-1} and at a pressure of *ca.* 6 mTorr, conditions similar to previously displayed data. The Daylight laser has a linewidth of *ca.* 2 MHz as determined previously using Lamb dip spectroscopy.[16,19] Therefore the velocity group pumped by this laser is larger than that pumped by the Maxion laser. Again the optical Bloch equations were solved to model the behaviour of the system and the resulting simulation is shown in the inset to Fig. 12. Once more the agreement is good.

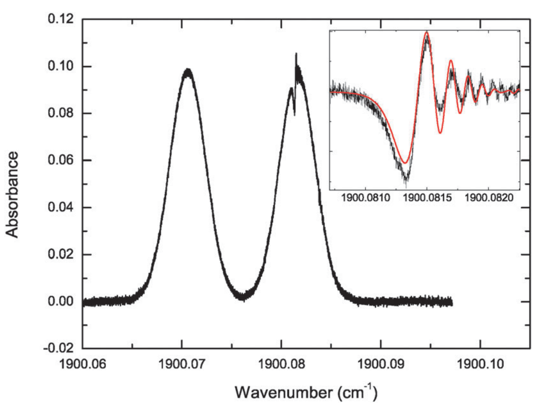

Fig. 12 The absorption signal seen when a separate fixed frequency (Daylight) QCL is used to pump a single velocity group within the $R(6.5)_{\frac{1}{2}}$ transition. The pumped velocity group has a non-zero, small velocity component in the direction of propagation and so the dip caused by the hole burnt into the ground state population is not centered within the Doppler profile. Inset is shown a fit to the rapid passage oscillations using the optical Bloch equations.

4 Conclusions

The linewidth of a high power continuous wave quantum cascade laser was determined to be 800 $\pm$ 60 kHz through Lamb dip spectroscopy. The effects of rapid passage on Lamb dips were investigated and initially increasing chirp rates were found to favour population transfer, in good agreement with Hamadani's work on adiabatic rapid passage with a chemical laser in which the efficiency of the population transfer from the initial state into the excited vibrational state can be controlled by the laser chirp rate.[18] Whilst amplification was not observed, population transfer efficiencies of up to 35% were measured which could be controlled by the laser chirp rate. By increasing the chirp rate further, rapid passage effects have, for the first time, been demonstrated in a Lamb dip experiment using a narrow linewidth, high power single mode quantum cascade laser. The absorption signals were observed to display asymmetric lineshapes, owing to the rate at which the probe laser is chirped through resonance with previously pumped velocity groups. If this rate is much higher than the rate at which the upper state is depopulated then an asymmetric lineshape results reflecting the degree of initial population transfer. This same condition is also necessary to observe rapid passage oscillations on the Lamb dip. The oscillations were only seen due to the narrow laser linewidth and were seen to be affected by the hyperfine splitting in the transition. Finally it was shown that it was possible to separate the asymmetry effect from the rapid passage oscillations by pumping a single velocity group using a second laser at a fixed frequency.

Acknowledgements

This work is conducted under the Engineering and Physical Sciences Research Council programme grant EP/G00224X/1: New Horizons in Chemical and Photochemical Dynamics. J. Kirkbride would like to thank the EPSRC for the award of a postgraduate studentship.

References

1 R. Maulini, I. Dunayevskiy, A. Lyakh, A. Tsekoun, C. Patel, L. Diehl, C. Pflügl and F. Capasso, *Electron. Lett.*, 2009, **45**, 107.
2 S. Bartalini, S. Borri, P. Cancio, A. Castrillo, I. Galli, G. Giusfredi, D. Mazzotti, L. Gianfrani and P. De Natale, *Phys. Rev. Lett.*, 2010, **104**, 4.
3 R. F. Curl, F. Capasso, C. Gmachl, A. A. Kosterev, B. McManus, R. Lewicki, M. Pusharsky, G. Wysocki and F. K. Tittel, *Chem. Phys. Lett.*, 2010, **487**, 1–18.
4 Y. Yao, A. J. Hoffman and C. F. Gmachl, *Nat. Photonics*, 2012, **6**, 432–439.
5 M. T. McCulloch, G. Duxbury and N. Langford, *Mol. Phys.*, 2006, **104**, 2767–2779.
6 G. Duxbury, N. Langford, M. T. McCulloch and S. Wright, *Mol. Phys.*, 2007, **105**, 741–754.

7 R. J. Walker, J. H. van Helden, J. Kirkbride, E. A. McCormack, M. T. Bell, D. Weidmann and G. A. D. Ritchie, *Opt. Lett.*, 2011, **36**, 4725–4727.
8 E. A. McCormack, H. S. Lowth, M. T. Bell, D. Weidmann and G. A. D. Ritchie, *J. Chem. Phys.*, 2012, **137**, 034306.
9 G. Duxbury, J. F. Kelly, T. A. Blake and N. Langford, *J. Chem. Phys.*, 2012, **136**, 174318.
10 G. Duxbury, J. F. Kelly, T. A. Blake and N. Langford, *J. Chem. Phys.*, 2012, **136**, 174319.
11 W. Lamb, *Phys. Rev.*, 1964, **134**, A1429–A1450.
12 V. S. Letokhov, in *High-Resolution Laser Spectroscopy*, ed. K. Shimoda, Springer-Verlag, Berlin, 1976, vol. 12, p. 96.
13 N. Mukherjee, R. Go and C. K. N. Patel, *Appl. Phys. Lett.*, 2008, **92**, 111116.
14 L. Rothman, I. Gordon, A. Barbe, D. Benner, P. Bernath, M. Birk, V. Boudon, L. Brown, A. Campargue and J.-P. Champion, *J. Quant. Spectrosc. Radiat. Transfer*, 2009, **110**, 533–572.
15 N. Mukherjee and C. K. N. Patel, *Chem. Phys. Lett.*, 2008, **462**, 10–13.
16 G. Hancock, G. A. D. Ritchie, J.-P. van Helden, R. Walker and D. Weidmann, *Opt. Eng.*, 2010, **49**, 111121.
17 S. Bartalini, S. Borri, I. Galli, G. Giusfredi, D. Mazzotti, T. Edamura, N. Akikusa, M. Yamanishi and P. De Natale, *Opt. Express*, 2011, **19**, 17996–18003.
18 S. M. Hamadani, A. T. Mattick, N. A. Kurnit and A. Javan, *Appl. Phys. Lett.*, 1975, **27**, 21.
19 R. J. Walker, J. H. van Helden and G. A. D. Ritchie, *Chem. Phys. Lett.*, 2010, **501**, 20–24.